Report

Current Biology

A brainstem circuit for the expression of defensive facial reactions in rat

Graphical abstract

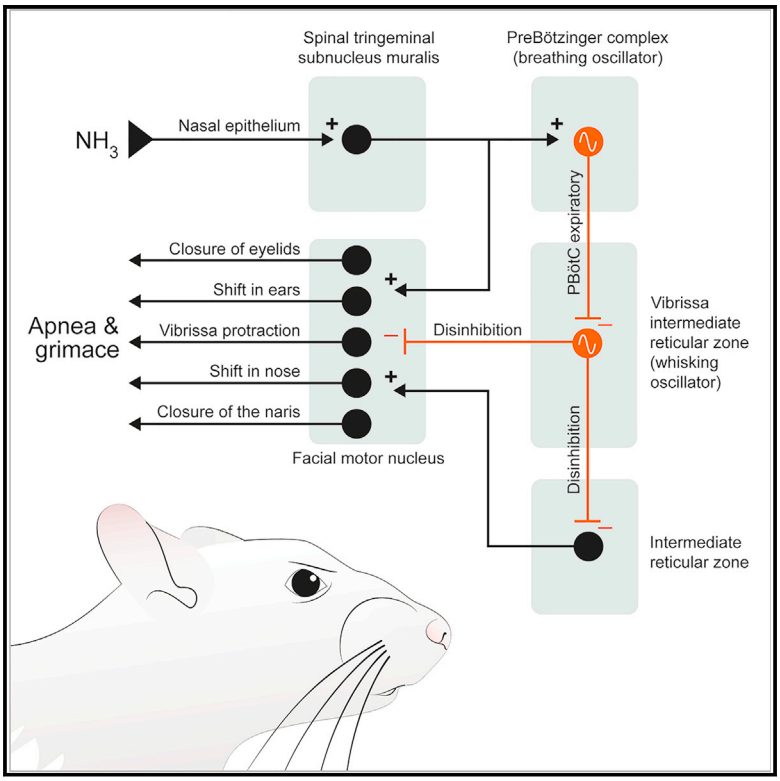

Highlights

- Chemoreceptors of nociceptive agents are known to reside in the nasal epithelium
- They activate trigeminal afferents that project to trigeminus subnucleus muralis
- Neurons in muralis both inhibit preBötzinger activity and drive facial motoneurons
- Activation of this pathway thus triggers an apneic reaction and triggers a grimace

Authors

Amalia Callado Pérez, Maxime Demers, Arash Fassihi, Jeffrey D. Moore, David Kleinfeld, Martin Deschênes

Correspondence

dk@physics.ucsd.edu (D.K.), martin.deschenes@fmed.ulaval.ca (M.D.)

In brief

Chemoreceptors in the nasal epithelium can trigger an apneic reaction and a grimace in response to airborne irritants. Callado Pérez et al. find that the underlying circuit does not involve olfaction. Rather, activation of neurons in the muralis subnucleus of the spinal trigeminal complex will inhibit the preBötzinger inhalation oscillator.

Callado Pérez et al., 2023, Current Biology *33*, 1–6
September 25, 2023
https://doi.org/10.1016/j.cub.2023.08.041

CellPress

Please cite this article in press as: Callado Pérez et al., A brainstem circuit for the expression of defensive facial reactions in rat, Current Biology (2023), https://doi.org/10.1016/j.cub.2023.08.041

Current Biology

CellPress

Report

A brainstem circuit for the expression of defensive facial reactions in rat

Amalia Callado Pérez,[1,2] Maxime Demers,[1] Arash Fassihi,[2] Jeffrey D. Moore,[3] David Kleinfeld,[2,4,5,*] and Martin Deschênes[1,*]

[1]Cervo Research Center, Université Laval, Québec City, Québec G1J 2R3, Canada
[2]Department of Physics, University of California, San Diego, La Jolla, CA 92093, USA
[3]Department of Biological Sciences, University of Southern California, Los Angeles, CA 90089, USA
[4]Department of Neurobiology, University of California, San Diego, La Jolla, CA 92093, USA
[5]Lead contact
*Correspondence: dk@physics.ucsd.edu (D.K.), martin.deschenes@fmed.ulaval.ca (M.D.)
https://doi.org/10.1016/j.cub.2023.08.041

SUMMARY

The brainstem houses neuronal circuits that control homeostasis of vital functions. These include the depth and rate of breathing[1,2] and, critically, apnea, a transient cessation of breathing that prevents noxious vapors from entering further into the respiratory tract. Current thinking is that this reflex is mediated by two sensory pathways. One known pathway involves vagal and glossopharyngeal afferents that project to the nucleus of the solitary tract.[3–5] Yet, apnea induced by electrical stimulation of the nasal epithelium or delivery of ammonia vapors to the nose persists after brainstem transection at the pontomedullary junction, indicating that the circuitry that mediates this reflex is intrinsic to the medulla.[6] A second potential pathway, consistent with this observation, involves trigeminal afferents from the nasal cavity that project to the muralis subnucleus of the spinal trigeminal complex.[7,8] Notably, the apneic reflex is not dependent on olfaction as it can be initiated even after disruption of olfactory pathways.[9] We investigated how subnucleus muralis cells mediate apnea in rat. By means of electrophysiological recordings and lesions in anesthetized rats, we identified a pathway from chemosensors in the nostrils through the muralis subnucleus and onto both the preBötzinger and facial motor nuclei. We then monitored breathing and orofacial reactions upon ammonia delivery near the nostril of alert, head-restrained rats. The apneic reaction was associated with a grimace, characterized by vibrissa protraction, wrinkling of the nose, and squinting of the eyes. Our results show that a brainstem circuit can control facial expressions for nocifensive and potentially pain-inducing stimuli.

RESULTS

Ammonia serves as the nociceptive agent in our study. In humans, when ammonia is delivered near the nose of an awake individual, it triggers an apneic reaction together with facial protective reflexes. The nares close, the nose wrinkles, and the eyes squint.[10] These facial reactions are clearly seen in power weightlifters who sniff ammonia salts just before a lift. We thus employ the ammonia test as a tool to identify the circuitry involved in ammonia-induced apnea in rat.

Our first experiments made use of micropipettes containing Chicago sky blue to map the receptive field of cells in the muralis subnucleus (8 rats). This area lies within the medullary dorsal horn. This area is a known target of the trigeminal anterior ethmoid nerve whose stimulation can trigger apnea; reviewed by Panneton and Gan.[9] The physiological sensory properties of the subnucleus muralis, however, have not been charted. We made one descent per rat, and the location of each cell was registered with respect to blue spots made at the start and end of each descent. We found that muralis cells respond to mechanical stimulation of the nasal and oral epithelia, whereas most of the nearby cells in the interpolaris and caudalis subnuclei of the sensory trigeminal complex respond to mechanical stimulation of the vibrissae or the mystacial fur (Figure S1).

In additional experiments, we recorded the response of muralis cells to puffs of ammonia vapors delivered near the nostrils and labeled the recording site with Chicago sky blue. We tested ten cells (10 rats) that were driven by stimulation of nose entrance with ammonia. These cells responded with a strong increase in their spike rate (Figures 1A, 1B, S2A, and S2B). They were all located in a 300-μm-thick zone at the ventral lateral border of the muralis subnucleus (Figures S2C and S2D). Together, these results are in concurrence with those of prior studies reporting that muralis cells receive input from the anterior ethmoidal nerve that innervates the entrance of the nares and the nasal mucosa; reviewed by Panneton et al.[11]

We delivered ammonia vapors directly into the nasal cavity to selectively activate ammonia-sensitive trigeminal afferents (Figures 1C–1F). Rats were tracheotomized, the left nasal cavity was opened by removing part of the nasal bone in front of the nasofrontal suture, and a cotton ball was inserted into the caudal part of the nasal cavity to block access of vapor to the nasopharynx; this is necessary as prior work showed that laryngeal

Please cite this article in press as: Callado Pérez et al., A brainstem circuit for the expression of defensive facial reactions in rat, Current Biology (2023), https://doi.org/10.1016/j.cub.2023.08.041

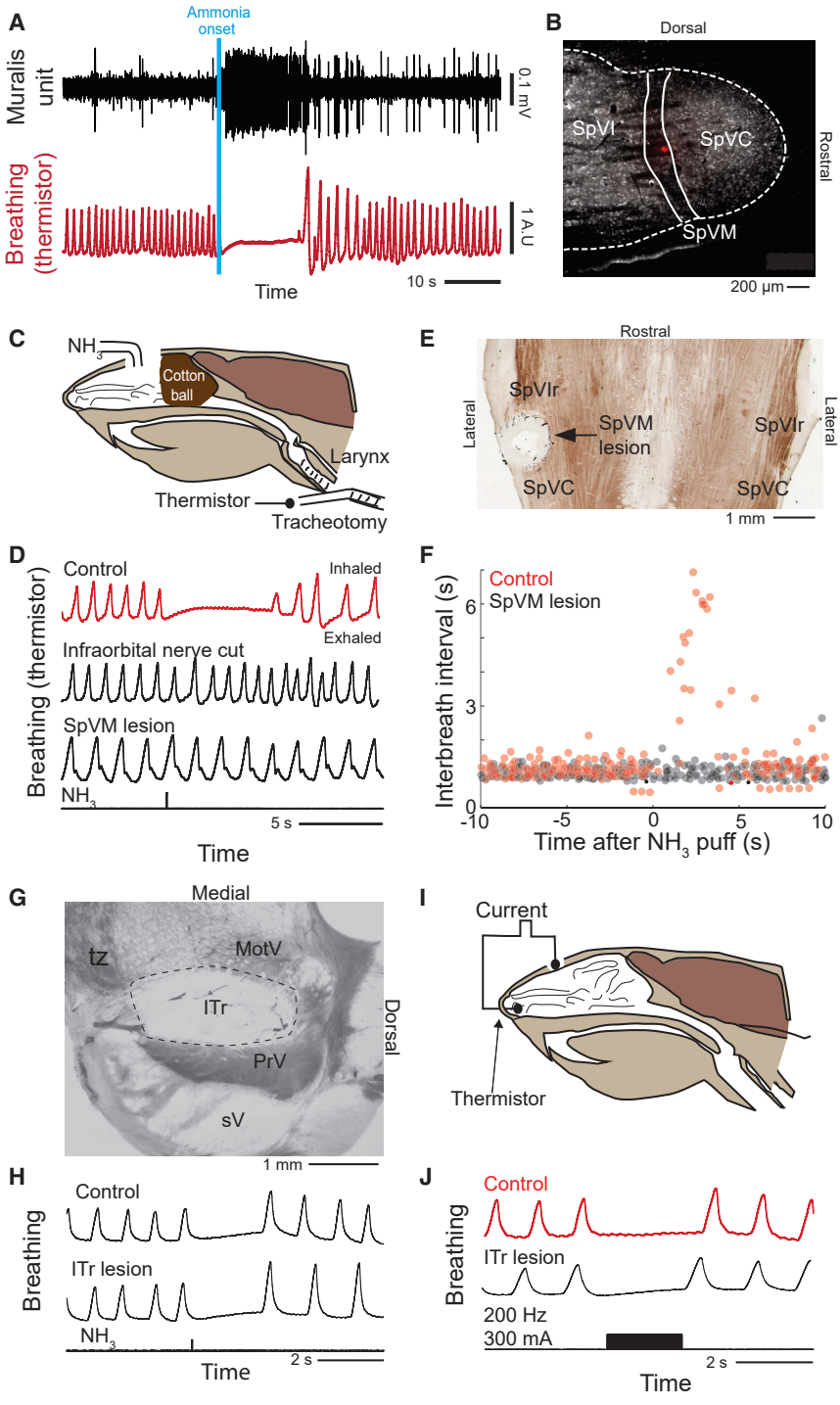

Figure 1. Delivery of a puff of ammonia vapor into the nasal cavity induces apnea

See Figures S1 and S2 for anatomical substrate of these data and Figure S2 for spiking responses in the spinal trigeminal subnucleus muralis.

(A) Schema of the general experimental approach with head-fixed, anesthetized, and tracheotomized rat; see text for details.

(B) Representative examples of an apneic reaction (control) and abolition of the apneic reaction following infraorbital nerve cut or lesion of subnucleus muralis (C).

(C) Representative histology after lesion of spinal trigeminal subnucleus muralis. Abbreviations: SpVC, spinal trigeminal subnucleus caudalis; SpVIc, caudal aspect of the spinal trigeminal subnucleus interpolaris; SpVIr, rostral aspect of the spinal trigeminal subnucleus interpolaris; SpVM, spinal trigeminal subnucleus muralis.

(D) Prolongation of the respiratory period induced by ammonia is abolished after lesion of subnucleus muralis.

(E) Representative histology after an extensive electrolytic lesion of the intertrigeminal region (ITr). Abbreviations: MotV, trigeminal motor nucleus; PrV, principal trigeminal sensory nucleus; sV, sensory root of the trigeminal nerve; tz, trapezoid body.

(F) Delivery of ammonia vapors at the entrance of the nares provokes an apneic reaction that persists after an extensive electrolytic lesion of the ITr.

(G) Schema of the general experimental approach for electrical stimulation of the nasal epithelium.

(H) Electrical stimulation of the nasal epithelium provokes an apneic reaction which persists after an extensive electrolytic lesion of the ITr.

and lung irritation produce apnea by non-trigeminal pathways.[12] To monitor breathing, a thermistor was paced in front of the nose (Figure 1C). A puff of ammonia vapors (1 s pulse of 30% [v/v] concentrated ammonia in water) was delivered to the nasal cavity to elicit an apneic reaction (Figure 1D). In contrast, apnea did not occur after transection of the left intraorbital nerve, which contains the ethmoidal nerve (6 rats), thus confirming the trigeminal origin of the reflex (Figure 1D). Electrolytic lesion of the left subnucleus muralis (5 rats) prevented trigeminally induced apnea (Figures 1E and 1F) but did not block the apneic reflex elicited by ammonia delivery to the trachea or to the right naris. The apneic reaction persisted after an extensive lesion of the left intertrigeminal region (ITr), i.e., the upper brainstem region located between the principal sensory trigeminal nucleus and the trigeminal motor nucleus (3 rats) (Figures 1G and 1H); this lesion severs descending projections from the pontine respiratory group. Apnea elicited by either ammonia or electrical stimulation of the nasal epithelium displayed similar characteristics (cf. Figure 1C and 1D with 1I and 1J); when tested with ammonia stimulation it was prevented by lesion of subnucleus muralis (Figure 1D) but persisted after lesion of the ITr (Figure 1J). These results both confirm those of a prior study[6] and substantially extend that work. Our new data show that trigeminally induced apnea is mediated by direct projections from the muralis/caudalis subnuclei to the medullary respiratory centers.

Using the above-described preparation, we recorded neuronal activities in the ventral respiratory group upon delivery of ammonia vapors into the nasal cavity (4 rats) (Figure 2A).

Please cite this article in press as: Callado Pérez et al., A brainstem circuit for the expression of defensive facial reactions in rat, Current Biology (2023), https://doi.org/10.1016/j.cub.2023.08.041

CellPress

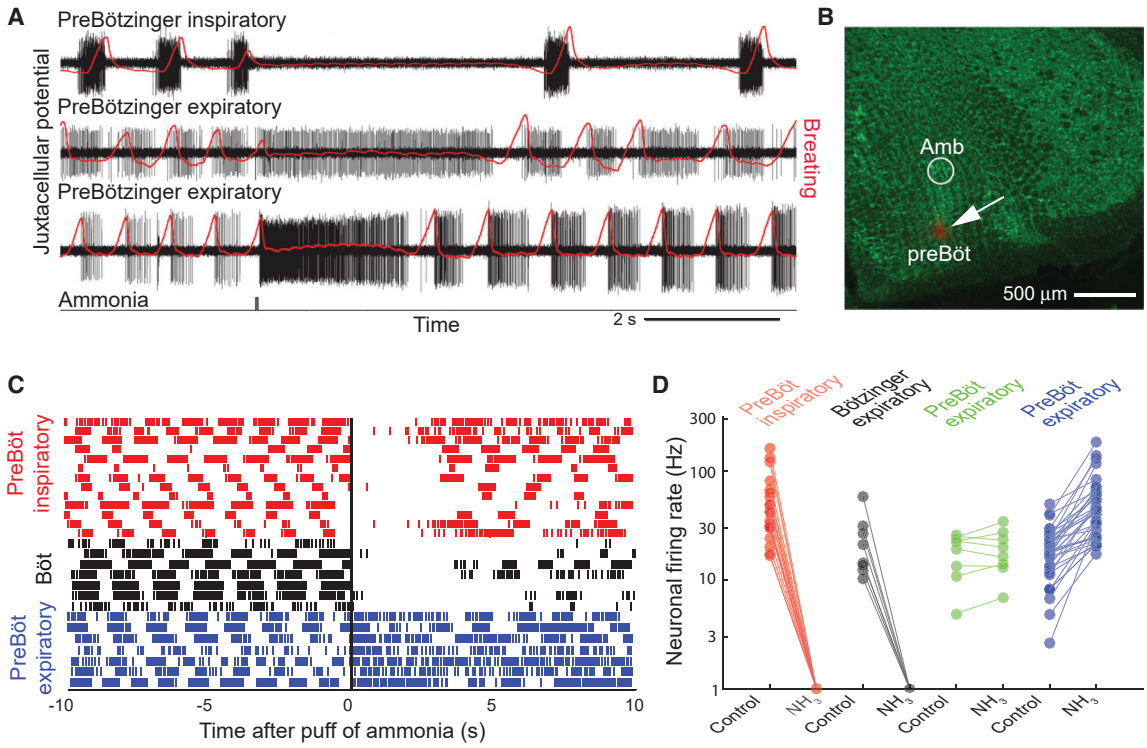

Figure 2. Change in firing rate of neurons of the ventral respiratory group upon delivery of ammonia vapors into the nasal cavity

(A) Representative responses of inspiratory and expiratory preBötzinger cells to a puff of ammonia. The red trace is the breathing signal recorded with a thermistor.

(B) Deposit of Chicago sky blue at the recording site in the preBötzinger complex.

(C) Representative raster plots of spiking by Bötzinger and preBötzinger cells before and after the ammonia puff.

(D) Plots of firing rate of Bötzinger and preBötzinger cells before and after the ammonia puff. While all inspiratory cells stop firing, expiratory cells display either no significant change (green dots, $p < 0.05$) or a marked increase in rate (black dots, $p < 0.05$).

Starting at the caudal edge of the facial nucleus, we made a series of descents spaced by 150 µm rostrocaudally and labeled the recording sites with Chicago sky blue (Figure 2B). We found that ammonia vapor inhibits expiratory Bötzinger cells and inspiratory preBötzinger cells (Figures 2C and 2D). In contrast, a majority of expiratory preBötzinger neurons (83%, 39 out of 47 cells) with rhythmic or sparse discharges significantly increased their firing rate (t test; $p < 0.05$) (Figure 2D).

A puff of ammonia vapor delivered near the nostril of an anesthetized rat induces an apneic reaction associated with closure of the naris.[13] In the alert head-restrained rat, this apneic reaction is also associated with bilateral protraction of the vibrissae; see Figure 1 in Moore et al..[14] In that same prior study, facial reactions were not documented. We thus monitored facial expressions in alert head-restrained rats upon delivery of ammonia vapor versus delivery of air as a control (4 rats) (Figure 3A and Videos S1 and S2) (STAR Methods). We observed that a puff of ammonia vapor prompts an apneic reaction (Figures 3B and 3C) that is associated with forward translation of the mystacial pad, wrinkling of the nose, squinting of the eyes, and curling of the ears (Figure 3A). This disgust-like grimace implies the co-activation of facial motoneurons that control movement of the vibrissae (Figure 3D), closure of the eyelids (Figure 3E), ear displacement (Figure 3F), and repositioning of the nose (Figures 3G and 3H) that results in closure of the nares. When the data for the change in facial expression of the vibrissae, eyelid, and nose were plotted with respect to the first breath after the puff of ammonia, rather than the onset time, we find that the grimace starts prior to the breath (Figure S3). This is consistent with a response driven by chemoreceptors in the nose rather than a response mediated by the olfactory bulb.

DISCUSSION

The present study uncovered a brainstem circuit through which delivery of noxious stimuli to the nose triggers apnea (Figures 1 and 2) and defensive facial reflexes (Figure 3). Prior studies showed that nasal stimulation with ammonia vapors activates medullary neurons that co-express the AMPA glutamate receptor subunits,[15] including those in the Kölliker-Fuse nucleus and the intertrigeminal region,[16,17] and that bilateral microinjection of lidocaine at the location of spinal trigeminal subnucleus muralis blocks ammonia-induced apnea in anesthetized rats.[18] Here, we show that ammonia-sensitive subnucleus muralis cells induce apnea by subsequently exciting preBötzinger expiratory neurons (Figure 2), most of which are GABAergic,[19] albeit only 10% of the GABAergic population.[20]

The motoneurons for the apneic reactions (Figure 3) reside in the dorsolateral and lateral sectors of the facial nucleus,[13,21,22] which receives projections from the glutamatergic cells of the

Please cite this article in press as: Callado Pérez et al., A brainstem circuit for the expression of defensive facial reactions in rat, Current Biology (2023), https://doi.org/10.1016/j.cub.2023.08.041

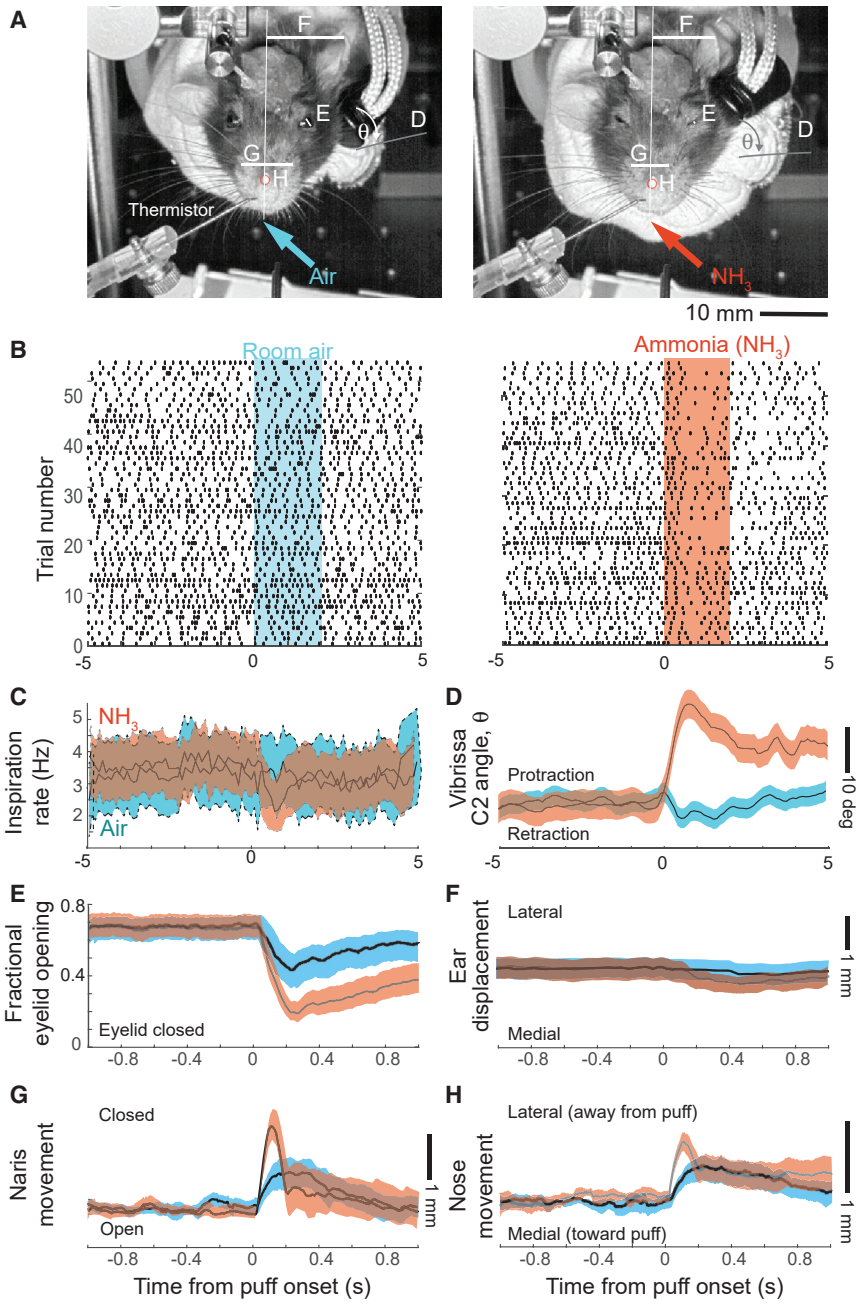

Figure 3. Facial reactions induced by delivery of ammonia vapors to the right nostril of a head-restrained rat

See Figure S3 for comparison with response locked to onset of the first breath after the stimulus.

(A) Frames from a video sequence that lie before and after the application of an ammonia vapor. Lines indicate how the motion of facial features were parameterized; the letters refer to panels in this figure. See STAR Methods for a detailed description of the analysis; note that vibrissae were measured with a separate line-scan camera from above. For representative video recordings, see Videos S1 and S2.

(B) Representative inspiratory events to the last air puff preceding delivery of room air or ammonia vapor; data across all rats.

(C–H) Delivery of an ammonia puff prompts a short apneic reaction (C) together with vibrissa protraction (D), closure of the eyelids (E), curling of the ears (F), and wrinkling of the nose (G and H). Note that ear displacement following ammonia delivery did not reach significance because movement of the rat in the sac masked landmarks used to estimate ear motion in about 50% of the trials (32 air puffs and 35 NH_3 puffs). Significance levels $p < 0.05$.

vibrissa intermediate reticular formation (vIRt).[22] This suggests that ammonia delivery may prompt a grimace by co-activating facial motoneurons innervated by glutamatergic vIRt cells, as opposed to the GABAergic vIRt cells that drive rhythmic whisking.[21,22]

The proposed brainstem circuitry that underlies facial reactions triggered by ammonia delivery to the nostrils of an awaked rat is summarized in Figure 4. Axons of ammonia-responsive primary afferents in the nasal epithelium travel through the infraorbital nerve and terminate in the muralis division of the sensory trigeminal complex. Glutamatergic muralis cells serve as both premotor neurons and secondary sensory neurons. One pool of neurons projects directly to the facial nucleus and activates motoneurons that close the nares (Figure 3G). In parallel, another pool projects to the preBötzinger complex, where they excite GABAergic expiratory cells. Activation of these GABAergic neurons should inhibit glycinergic vIRt neurons that serve to drive vibrissa protraction through the inhibition of facial motoneurons. Thus, the disinhibition leads to sustained protraction of the vibrissae (Figure 3D).[22] The net result is a grimace-like disgust reaction (Figure 3A).

We used the ammonia test as a tool to identify the circuit and mechanisms through which afferents from the nasal cavity trigger reflexive apnea together with defense reactions. It is worth noting that similar grimacing reactions are triggered by aversive, yet non painful stimuli, e.g., disgust reaction to some food or to shocking situations. An intriguing possibility is that the same pool of IRt glutamatergic cells may drive facial reactions in other nocifensive behavioral contexts. Identifying brainstem afferents that drive these IRt glutamatergic cells would be a crucial step toward this goal.

The breathing oscillator serves to directly entrain the rhythmic output of the oscillator for whisking[13,14,22,23] and is likely to entrain the yet-to-be-identified oscillators for licking and lapping,[24] nose twitching,[25,26] and head rocking.[26,27] There is thus a loss of coordination among orofacial motor actions[28,29] during apnea. This suggests that nocifensive odorants and less volatile chemicals, which are part of the natural weapons and defenses in the animal kingdom, play a debilitating role beyond

Please cite this article in press as: Callado Pérez et al., A brainstem circuit for the expression of defensive facial reactions in rat, Current Biology (2023), https://doi.org/10.1016/j.cub.2023.08.041

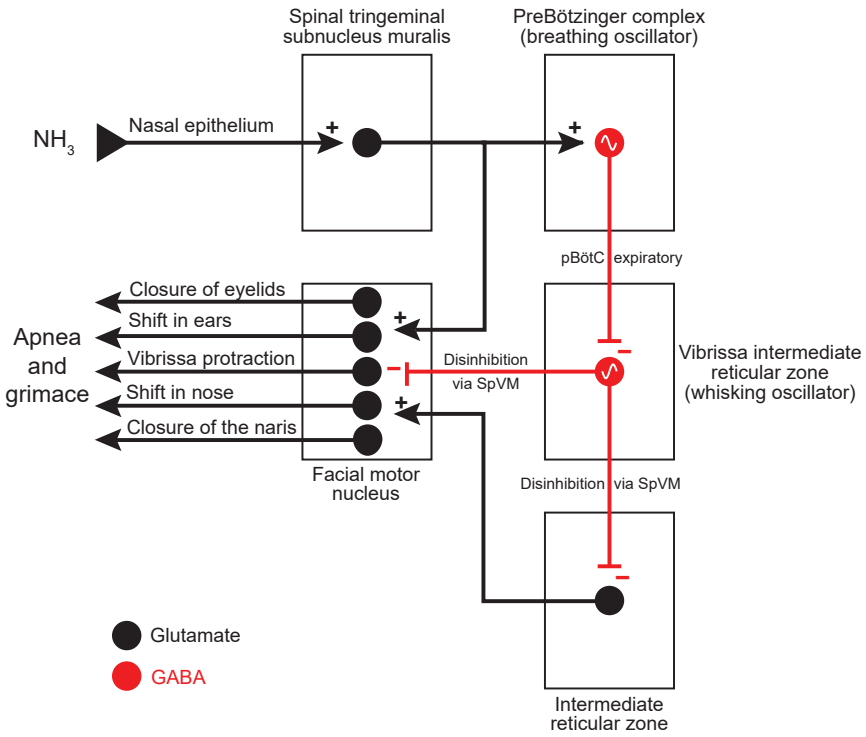

Figure 4. Wiring connections for the grimacing reaction induced by delivery of ammonia vapors near the nose of a rat

Ammonia activates a pool of excitatory spinal trigeminal subnucleus muralis cells that project to the facial nucleus and prompt closure of the nares, and another pool of inhibitory cells that project to the expiratory cells of the preBötzinger complex. The expiratory cells within the preBötzinger complex are glycinergic and are likely to inhibit the whisking oscillator (vIRt), which normally fires in a sustained manner. Inhibition of glycinergic vIRt cells disinhibits IRt glutamatergic cells (red arrow) which project to the motoneurons that control facial pad muscle, hence a grimace.

apnea per se. Although our current data and past results refer to studies on rodent subjects, the common neuronal architecture of the brainstem across mammalian species suggests that the circuitry for the apneic response will be common from mice to humans.

STAR★METHODS

Detailed methods are provided in the online version of this paper and include the following:

- KEY RESOURCES TABLE
- RESOURCE AVAILABILITY
  - Lead contact
  - Materials availability
  - Data and code availability
- EXPERIMENTAL MODEL AND SUBJECT DETAILS
  - Experimental subjects
  - Surgeries
- METHOD DETAILS
  - Apnea induced by delivery of ammonia vapors within the nasal cavity
  - Apnea induced by delivery of ammonia vapors near the nostrils
  - Electrophysiology and lesions
  - Video monitoring of facial expressions
  - Histology
  - Data analysis

SUPPLEMENTAL INFORMATION

Supplemental information can be found online at https://doi.org/10.1016/j.cub.2023.08.041.

ACKNOWLEDGMENTS

We thank Anastasia Kurnikova for assistance with preliminary experiments, Nicole Mercer Lindsay for assistance with analysis, Beth Friedman for discussion and commentary on the manuscript, Harvey Karten and Jun Takatoh for discussions, and Julia Kuhl for design of the graphical abstract. Supported by the National Institutes of Health (grants NS107466 and NS097265) and the Canadian Institutes of Health Research (grant MT-5877).

AUTHOR CONTRIBUTIONS

Conceived and designed the experiments: M. Deschênes and D.K. Performed the experiments: A.C.P., M. Demers, and M. Deschênes. Analyzed the data: M. Demers, A.F., and D.K. Contributed materials and analysis tools: M. Deschênes, D.K., and J.D.M. Wrote the paper: M. Deschênes with revisions by D.K.

DECLARATION OF INTERESTS

The authors declare no competing interests.

Received: April 21, 2023
Revised: August 8, 2023
Accepted: August 15, 2023
Published: September 12, 2023

REFERENCES

1. Doi, A., and Ramirez, J.M. (2008). Neuromodulation and the orchestration of the respiratory rhythm. Respir. Physiol. Neurobiol. *164*, 96–104.
2. Del Negro, C.A., Funk, G.D., and Feldman, J.L. (2018). Breathing matters. Nat. Rev. Neurosci. *19*, 351–367. https://doi.org/10.1038/s41583-018-0003-6.
3. Patrickson, J.W., Smith, T.E., and Zhou, S.-S. (1991). Afferent projections of the superior and recurrent laryngeal nerves. Brain Res. *539*, 169–174.

4. Furusawa, K., Yasuda, K., Okuda, D., Tanaka, M., and Yamaoka, M. (1996). Central distribution and peripheral functional properties of afferent and efferent components of the superior laryngeal nerve: morphological and electrophysiological studies in the rat. J. Comp. Neurol. *375*, 147–156.
5. Pascual-Font, A., Hernández-Morato, I., McHanwell, S., Vázquez, T., Maranillo, E., Sañudo, J., and Valderrama-Canales, F.J. (2011). The central projections of the laryngeal nerves in the rat. J. Anat. *219*, 217–228.
6. Panneton, W.M., Gan, Q., and Sun, D.W. (2012). Persistence of the naso-trigeminal reflex after pontomedullary transection. Respir. Physiol. Neurobiol. *180*, 230–236.
7. Matthews, D.W., Deschênes, M., Furuta, T., Moore, J.D., Wang, F., Karten, H.J., and Kleinfeld, D. (2015). Feedback in the brainstem: An excitatory disynaptic pathway for control of whisking. J. Comp. Neurol. *523*, 921–942.
8. Anton, F., and Peppel, P. (1991). Central projections of trigeminal primary afferents innervating the nasal mucosa: a horseradish peroxidase study in the rat. Neuroscience *41*, 617–628.
9. Panneton, W.M., and Gan, Q. (2020). The mammalian diving response: Inroads to its neural control. Front. Neurosci. *14*, e00524.
10. Wood, R.W. (1979). Behavioral evaluation of sensory irritation evoked by ammonia. Toxicol. Appl. Pharmacol. *50*, 157–162.
11. Panneton, W.M., Pan, B., and Gan, Q. (2017). Somatotopy in the medullary dorsal horn as a basis for orofacial reflex behavior. Front. Neurol. *8*, e522.
12. Panneton, W.M. (1990). Controlled bradycardia induced by nasal stimulation in the muskrat, Ondatra zibethicus. J. Auton. Nerv. Syst. *30*, 253–263.
13. Deschênes, M., Takatoh, J., Kurnikova, A., Moore, J.D., Demers, M., Elbaz, M., Furuta, T., Wang, F., and Kleinfeld, D. (2016). Inhibition, not excitation, drives rhythmic whisking. Neuron *90*, 374–387.
14. Moore, J.D., Deschênes, M., Furuta, T., Huber, D., Smear, M.C., Demers, M., and Kleinfeld, D. (2013). Hierarchy of orofacial rhythms revealed through whisking and breathing. Nature *497*, 205–210.
15. McCulloch, P.F., DiNovo, K.M., Westerhaus, D.J., Vizinas, T.A., Peevey, J.F., Lach, M.A., and Czarnocki, P. (2013). Trigeminal medullary dorsal horn neurons activated by nasal stimulation coexpress AMPA, NMDA and NK1 receptors. ISRN Neurosci. *2013*, e152567.
16. Chamberlin, N.L., and Saper, C.B. (1994). Topographic organization of respiratory responses to glutamate microstimulation of the parabrachial nucleus in the rat. J. Neurosci. *14*, 6500–6510.
17. Dutschmann, M., and Herbert, H. (1996). The Kölliker-Fuse nucleus mediates the trigeminally induced apnea in the rat. Neuroreport *7*, 1432–1436.
18. Panneton, W.M., and Yavari, P. (1995). Medullary dorsal horn relay for the cardiorespiratory responses by stimulation of the nasal mucosa in the muskrat Ondatra zibethicus: Evidence for excitatory amino acid transmission. Brain Res. *691*, 37–45.
19. Yang, C.F., and Feldman, J.L. (2018). Efferent projections of excitatory and inhibitory preBötzinger complex neurons. J. Comp. Neurol. *526*, 1389–1402.
20. Baertsch, N.A., Baertsch, H.C., and Ramirez, J.M. (2018). The interdependence of excitation and inhibition for the control of dynamic breathing rhythms. Nat. Commun. *9*, e843.
21. Deschênes, M., Haidarliu, S., Demers, M., Moore, J., Kleinfeld, D., and Ahissar, E. (2015). Muscles involved in naris dilation and nose motion in rat. Anat. Rec. *298*, 546–553.
22. Takatoh, J., Prevosto, V., Thompson, P.M., Lu, J., Chung, L., Harrahill, A., Li, S., Zhao, S., He, Z., Golomb, D., et al. (2022). The whisking oscillator circuit. Nature *609*, 560–568.
23. Golomb, D., Moore, J.D., Fassihi, A., Takatoh, J., Prevosto, V., Wang, F., and Kleinfeld, D. (2022). Theory of hierarchically organized neuronal oscillator dynamics that mediate rodent rhythmic whisking. Neuron *110*, 3833–3851.e22.
24. Dempsey, B., Sungeelee, S., Bokiniec, P., Chettouh, Z., Diem, S., Autran, S., Harrell, E.R., Poulet, J.F.A., Birchmeier, C., Carey, H., et al. (2021). A medullary centre for lapping in mice. Nat. Commun. *12*, e6307.
25. Kurnikova, A., Deschênes, M., and Kleinfeld, D. (2019). Functional brain stem circuits for control of nose motion. J. Neurophysiol. *121*, 205–217.
26. Kurnikova, A., Moore, J.D., Liao, S.-M., Deschênes, M., and Kleinfeld, D. (2017). Coordination of orofacial motor actions into exploratory behavior by rat. Curr. Biol. *27*, 688–696.
27. Liao, S.-M., and Kleinfeld, D. (2023). A change in behavioral state switches the pattern of motor output that underlies rhythmic head and orofacial movements. Curr. Biol. *33*, 1951–1966.e6.
28. Moore, J.D., Kleinfeld, D., and Wang, F. (2014). How the brainstem controls orofacial behaviors comprised of rhythmic actions. Trends Neurosci. *37*, 370–380.
29. Kleinfeld, D., Deschênes, M., Wang, F., and Moore, J.D. (2014). More than a rhythm of life: Breathing as a binder of orofacial sensation. Nat. Neurosci. *17*, 647–651.
30. Ahrens, K.F., and Kleinfeld, D. (2004). Current flow in vibrissa motor cortex can phase-lock with exploratory whisking in rat. J. Neurophysiol. *92*, 1700–1707.
31. Moore, J.D., Mercer Lindsay, N., Deschênes, M., and Kleinfeld, D. (2015). Vibrissa self-motion and touch are encoded along the same somatosensory pathway from brainstem through thalamus. PLoS Biol. *13*, e1002253.
32. McAfee, S.S., Ogg, M.C., Ross, J.M., Liu, Y., Fletcher, M.L., and Heck, D.H. (2016). Minimally invasive highly precise monitoring of respiratory rhythm in the mouse using an epithelial temperature probe. J. Neurosci. Methods *263*, 89–94.
33. Hill, D.N., Curtis, J.C., Moore, J.D., and Kleinfeld, D. (2011). Primary motor cortex reports efferent control of vibrissa position on multiple time scales. Neuron *72*, 344–356.
34. Aljadeff, J., Lansdell, B.J., Fairhall, A.L., and Kleinfeld, D. (2016). Analysis of neuronal spike trains, deconstructed. Neuron *91*, 221–259.

Please cite this article in press as: Callado Pérez et al., A brainstem circuit for the expression of defensive facial reactions in rat, Current Biology (2023), https://doi.org/10.1016/j.cub.2023.08.041

STAR★METHODS

KEY RESOURCES TABLE

REAGENT or RESOURCE	SOURCE	IDENTIFIER
Chemicals, peptides, and recombinant proteins		
Ammonia solution 32%	Millipore Sigma	Cat no. 1054261011
Isoflurane	Henry Schein	Cat no. 1182097
Ketamine, injection	Zoetis	Cat no. 40027676
Xylazine, injection	AnaSed	Cat no. (01)00359399110204
Buprenorphine Hydrochloride, injection	Par Pharmaseutical	Cat no. 110483373347
Silicone elastomer	WPI	Kwik-Cast
Mouse anti-GFP antibody	Abcam	Cat no. ab1218
Chicken anti-GFP antibody	Abcam	Cat no. ab13970
Rabbit anti-GFP antibody	Abcam	Cat no. ab290
Rabbit anti-NeuN antibody	Millipore Sigma	Cat no. ABN78
Goat anti-choline acetyltransferase antibody	Millipore Sigma	Cat no. AB144P
Goat anti-rabbit IgG - Alexa 594	Invitrogen	Cat no. A11037
Donkey anti-chicken IgG - Alexa 488	Invitrogen	Cat no. A78948
rabbit anti-goat IgG - horseradish peroxidase	Millipore Sigma	Cat no. AP106P
Biotinylated anti-rabbit IgG	Vector Labs	Cat no. BA-1100
Biotinylated anti-mouse IgG	Vector Labs	Cat no. BA-9200
Avidin/biotin complex	Vector Labs	Vectastain ABC kit
SG peroxidase substrate	Vector Labs	Cat no. SK4705
Streptavidin, horseradish peroxidase conjugate	Millipore Sigma	Cat no. OR03L
Diaminobenzidine	Millipore Sigma	Cat no. D12384
Experimental models: Organisms/strains		
Rat: Long-Evans	Charles River Laboratories	N/A
Software and algorithms		
MATLAB	MathWorks	N/A
LabChart	AD Instruments	N/A
ProAnalyst motion analysis software	Xcitex Inc	N/A
Other		
CCD camera	Basler	Cat no. a602f
PowerLab	AD Instruments	Cat no. 16/35
Current stimulator	A-M Systems	Cat no. 2100
NTS thermistors	Measurement Specialities	Cat no. MEAS-G22K7MCD419
Piezoelectric film	Measurement Specialities	Cat no. LDT1 028K

RESOURCE AVAILABILITY

Lead contact

Further information and requests for resources and reagents should be directed to and will be fulfilled by Prof. David Kleinfeld (dk@physics.ucsd.edu).

Materials availability

This study did not generate any new unique materials.

Please cite this article in press as: Callado Pérez et al., A brainstem circuit for the expression of defensive facial reactions in rat, Current Biology (2023), https://doi.org/10.1016/j.cub.2023.08.041

Data and code availability

The datasets supporting the current study, and an associated "read me" file, will be available at https://dandiarchive.org/dandiset/000624 upon publication. The code for the analysis will be available upon publication at https://github.com/Rhythm-n-Rodents/Muralis-defensive-facial-reactions.

EXPERIMENTAL MODEL AND SUBJECT DETAILS

Experimental subjects

Experiments were carried out in Long Evans rats of both sexes (250–350 g in mass), according to the National Institutes of Health Guidelines. All experiments were approved by the Institutional Animal Care and Use Committee at Laval University and the University of California, San Diego.

Surgeries

Surgeries were carried out under ketamine (90 mg/kg) plus xylazine (10 mg/kg) anesthesia. Injections were made intraperitonally with supplemental doses (20 mg/kg) given as needed. Body temperature was maintained at 37 C with a thermostatically controlled heating pad. Respiration was monitored with a cantilevered piezoelectric film (LDT1 028K; Measurement Specialties) resting on the rat's abdomen just caudal to the torso.

METHOD DETAILS

Apnea induced by delivery of ammonia vapors within the nasal cavity

To get access to the nasal cavity an opening was made in the left nasal bone rostral to the nasofrontal suture, and the dorsal aspect of the nasal epithelium was opened by cauterization. The nasal cavity caudal to the nasofrontal suture was clogged with small cotton balls to prevent ammonia vapors to reach the nasopharynx. Ammonia vapors were delivered directly into the nasal cavity via a glass pipette (tip diameter, 0.3 mm) connected to a pressure injector (Picospritzer, General Valve / Parker Hannifin). In some experiments rats were also tracheotomized to ensure the effect of ammonia was limited to stimulation of the nasal epithelium (4 rats). Finally, in additional experiments (4 rats) the right nostril was transiently clogged with a silicone elastomer (Kwik-Cast; WPI) to make sure the effect of ammonia was restricted to the left nostril. It is worth mentioning that repeated application of ammonia to the nasal epithelium leads to abundant mucus secretion that eventually prevents the activation of nasal chemoreceptors. Once the mucus was removed by aspiration, the ammonia-induced apnea recovered.

Apnea induced by delivery of ammonia vapors near the nostrils

In 10 rats we recorded the response of muralis cells to puffs of ammonia vapors (1 s pulse of 30% NH_3) delivered near the nostrils. Once we found muralis neurons that responded to mechanical stimulation of nose entrance, a puff of ammonia vapor was delivered to assess whether cells discharge during the apneic reaction. If they did, we retested the cells once every 10 min (three times). Time spacing ammonia delivery prevented the blockade of cell responses by mucus secretion. Thereafter the recording site was labeled by an iontophoretic application of Chicago Sky Blue (−10 μA; pulse width, 3 s; half duty cycle for 10 min). The rat was perfused, and histology was carried out as described below.

Electrophysiology and lesions

Single units were recorded with micropipettes (tip diameter: 1 μm) filled with either 0.5 M potassium acetate or 0.5 M potassium acetate and 2% (w/v) Chicago Sky Blue. In three rats subnucleus muralis was lesioned unilaterally by injecting direct current (3 mA, 5 s) through a tungsten electrode (tip diameter: 20 μm, de-insulated over a length of 1 mm).[30]

Video monitoring of facial expressions

Four Long Evans rats were implanted with a head restraint post.[31] They were placed inside a body-restraining cloth sack and rigid tube and habituated to the head fixation rig over several daily sessions until they displayed normal grooming and whisking and a complete lack of struggling. For the recording sessions all vibrissae except C2 or D2 were cut at the base under light isoflurane anesthesia. Movement of the intact vibrissa was monitored from above with a Basler A602f camera at a 250-Hz frame rate in which the output in a selected narrow band was converted to a line-scan.[14] A fast time response NTS thermistors (MEAS-G22K7MCD419, Measurement Specialities; Hampton, VA) was used to monitor breathing.[32] The probe was positioned at the entrance of the nares and respiratory signals were amplified with a bridge amplifier (band pass: 0.5–15 Hz). Finally, two tubes (inside diameter: 1 mm) were glued together and positioned in front of the snout to deliver one or 2 s puffs of air only or air saturated with 30% ammonia vapors. Puff delivery was controlled remotely by a solenoid valve. A Basler A602f camera equipped with a macro video zoom lens was used to record from above facial reactions (resolution: 120 μm/pixel and 100 frames/s). Respiratory signals from the thermistor were synchronized with video frames through a PCI-6024E acquisition board (National Instruments). They were sampled at 200 Hz and logged on a computer using the LabChart acquisition system (AD Instruments). Data were imported in MATLAB (MathWorks) and analysis was carried out using custom software.

Please cite this article in press as: Callado Pérez et al., A brainstem circuit for the expression of defensive facial reactions in rat, Current Biology (2023), https://doi.org/10.1016/j.cub.2023.08.041

Histology

Following perfusion brains were postfixed for 2 h, and cryoprotected overnight in 30% sucrose in PBS. Brains were cut at thickness of 60 μm on a freezing microtome. Labeled material was processed for either fluorescence or brightfield microscopy. For fluorescence microscopy, sections were immunoreacted with a chicken anti-GFP antibody (1:1000; Abcam), and a donkey anti-chicken Alexa 488 IgG (Abcam). NeuN immunostaining was carried out with a rabbit anti-NeuN antibody (1:1000; EM Millipore) and an anti-rabbit IgG conjugated to Alexa 594. For brightfield microscopy, sections were first counterstained for cytochrome oxidase, and then immunoreacted with a rabbit anti-GFP antibody (1:1000; Novus Biological), a biotinylated anti-rabbit IgG (1:200: Vector Labs), the avidin/biotin complex (Vectastain ABC kit, Vector Labs), and the SG peroxidase substrate (Vector Labs). In three rats, brainstem sections were first immunoreacted with a goat anti-choline acetyltransferase antibody (1:1000; Millipore Sigma) and a rabbit anti-goat IgG conjugated to horseradish peroxidase (Vector Labs), which was revealed with diaminobenzidine (brown reaction product). Sections were then immunoreacted with a mouse anti-GFP antibody (1:2000; Abcam), a biotinylated anti-mouse IgG, which was revealed with streptavidin horseradish peroxidase conjugate and the Ni-DAB substrate (black reaction product). Finally, the extent of electrolytic lesions was assessed on material stained with Neutral Red. Sections were scanned at a resolution of 0.5 μm/pixel (TissueScope LE; Huron Digital Pathology) and imported in Fiji or Photoshop for color and contrast adjustments.

Data analysis

We used MATLAB (MathWorks) code for data analysis.

Analysis of breathing and facial reactions to ammonia

We restricted our analysis to video trials that included 1s of recording both before and after the air-puff trigger signal. The vibrissa angle with respect to the face was tracked from high-speed video data using custom MATLAB routines, as described previously.[14] Similarly, individual breaths were detected in the pre-puff recording as described previously.[14] Briefly, thermistor signals were digitally band-pass filtered between 1 and 15 Hz, and breaths were segmented by phase resets of the Hilbert transform[33]. In post-puff recording segments, this same method was applied to identify candidate breaths. Since the post-puff breathing was temporarily arrhythmic, candidate breaths were accepted if they were > 100 ms and > 10% of the mean amplitude of the pre-puff breaths. In each trial, breathing and whisking signals were aligned to the air-puff onset and divided into non-overlapping 250 ms bins. To estimate the air-puff triggered average breathing rate and vibrissa position, the number of breaths per bin and the mean whisker position per bin were computed across all trials in all subjects. The 95% bootstrap confidence intervals for these metrics were estimated by resampling trials with replacement[34].

Facial reactions to ammonia delivery were tracked using ProAnalyst motion analysis software (Xcitex Inc.). Briefly, marks were inserted at relevant points on video frames and their position was tracked across 10 s, centered on the time of ammonia delivery. Each video was manually annotated to ensure accurate tracking.